Advanced Materials 26 (2014): 6447-6453

DOI: http://doi.org/10.1002/adma.201401603

DOI: 10.1002/((please add manuscript number))
Article type: Communication

Blue SHG Enhancement by Silver Nanocubes Photochemically Prepared on $RbTiOPO_4$ Ferroelectric Crystal

Laura Sánchez-García[1], *Mariola O Ramírez*[1], *Pablo Molina*[1], *Francisco Gallego-Gómez*[1], *Luis Mateos*[1], *Eduardo Yraola*[1], *Joan Carvajal*[2], *Magdalena Aguiló*[2], *Francesc Díaz*[2], *Carmen de las Heras*[1] *and Luisa E. Bausá*[1,*]

Laura Sánchez-García, Dr. Mariola O Ramírez, Dr. Pablo Molina, Dr. Francisco Gallego-Gómez, Dr. Luis Mateos, Eduardo Yraola, Prof. Carmen de las Heras, and Prof. Luisa E. Bausá
Dpto. Física de Materiales and Instituto Nicolás Cabrera, Universidad Autónoma de Madrid, Madrid, 28049, Spain
E-mail: luisa.bausa@uam.es

Dr. Joan Carvajal, Prof. Magdalena Aguiló and Prof. Francesc Díaz
Fisica i Cristal·lografia de Materials i Nanomaterials (FiCMA-FiCNA) and EMaS, Universitat Rovira i Virgili, 43005-Tarragona, Spain

Keywords: second harmonic generation, $RbTiOPO_4$, ferroelectric lithography, silver nanocubes, localized surface plasmon

Metallic nanoparticles are of enormous interest for a wide range of scientific and technologic applications such as chemical and biological sensors,[1-3] surface-enhanced spectroscopies,[4] photodetection and light harvesting[5, 6] and optical nanodevices.[7,8] In these systems the resonant excitation of local surface plasmons (LSP) can lead to a strong confinement of the incident electromagnetic field at the nanoparticle surface providing a means to significantly enhance the optical interactions at subwavelength scales.[9] The plasmon-resonance conditions depend on both size and geometry of the nanoparticles, which justifies the growing interest in the fabrication and control of different types of metallic nanoparticle morphologies.[10-12] Therefore, well-shaped nanoparticles with narrow size distribution are highly desirable for specific applications. In particular, edged morphologies like cubes or prisms lead to more intense near-field for better manipulation of the optical

properties of neighboring systems. For instance, silver nanocubes show exceptional capabilities for chemical sensing applications.[13] They have also been recently proven as valid nano-antennas for controlling the absorptivity of large surface areas showing the potential of monodisperse cubic metal nanostructures to engineer new metamaterials at large scales not reachable by top-down lithographic approaches.[14]

So far, different methods based on colloidal chemistry constitute the conventional routes for the fabrication of particles with different shapes.[15] These routes require high-quality nucleation seeds and capping agents to control the particle growth, among filtering or other size segregation to obtain acceptable monodispersity.

Here, we demonstrate the preparation of silver nanocubes exhibiting low (~10%) size dispersion by simple photochemical deposition on the polar surface of a ferroelectric crystal. Ferroelectric crystals, characterized by the presence of a spontaneous polarization in the ferroelectric phase, show high electro-optical, piezoelectric, pyroelectric and nonlinear coefficients useful in microelectronic and advanced photonics. Their applications involve non-volatile memories, piezoelectric actuators, ultrasound transducers, surface acoustic waves, as well as electro-optic, and nonlinear systems. [16] Additionally, polar surfaces of ferroelectric crystals allow polarization-mediated metallic deposition by photochemical reduction for simple, low-cost fabrication of metal nanoparticles and nanostructures. Indeed, the progress achieved so far in micro-engineering of ferroelectric domains facilitates the fabrication of templates with alternating surface charge on which domain-specific deposition of metals (silver, palladium, gold, platinum,..) has been demonstrated.[17,18] However, up to our knowledge, no regard was taken on the achievement of specific shapes or monodispersity for the obtained metal nanoparticles by using that procedure. Here, we have taken advantage of the particular crystal structure of a chosen ferroelectric, the rubidium titanyl phosphate $RbTiOPO_4$ (RTP), to favor photoinduced silver deposition in the form of nanocubes. RTP has

a *mm*2 point symmetry. Despite the twofold symmetry of RTP the projection of the crystal structure on the polar surface shows a multi-square-like grid atomic arrangement useful to fit the cubic structure of metallic silver. We demonstrate the direct synthesis of ~~nearly monodisperse~~ silver nanocubes with edge length of 57 ± 6 nm on the polar surface of RTP without further processing. The obtained nanocubes present three preferential directions, which can be related to the structure of the RTP polar surface suggesting epitaxial orientation.

On the other hand, due to its relatively large nonlinear coefficients, RTP has shown to be an efficient system for blue light generation by efficient quadratic frequency doubling processes.[19] Here, the plasmonic properties of the photo-deposited silver nanocubes on the polar surface of RTP are used to enhance the performance of the nonlinear frequency conversion in the blue spectral region, which is of technological interest in the context of nonlinear photonic nanodevices.

RTP is an isostructural of the titanyl phosphate family of ferroelectric compounds, the most renowned member of which is $KTiOPO_4$ (KTP), which offers some advantages over its KTP counterpart such as a higher optical damage threshold,[20] and lower coercive field (near 3 times lower than KTP),[21] which is crucial for domain structuring, especially in thick samples. In our work, direct electron beam writing (DEBW) has been used to fabricate periodic patterns of 180° ferroelectric domains in RTP as templates for the domain-selective photochemical deposition of silver nanostructures. DEBW has been chosen as a tool to reverse the spontaneous polarization in RTP, since it offers some interesting advantages (no previous masking process, micrometer and sub-micrometer control in large areas)[22, 23] over the previously used methods for polarization inversion in this system.[21, 24] One-dimensional ferroelectric domain structures with different periodicities (from 5 to 50 μm) and domain widths along the ***a*** direction ranging from 5 to 20 μm were obtained by DEBW on the ***c***-surface of RTP. The inverted domains crossed the whole sample thickness (1.3 mm) and

preserved their size and shape at both faces, being stable at least up to a monthly scale. The conditions and parameters of the irradiation processes are described at the experimental section. **Figure 1** (a) shows a differential interference contrast (DIC) microscopy image of one of the obtained periodically poled RTP consisting of inverted domains 10 μm width separated 30 μm. The image was obtained without the need of chemical etching. The presence of the antiparallel 180º domain structures fabricated in our RTP crystal was also confirmed by piezo-response force microscopy (PFM). Figure 1 (b) shows, as an example, the piezoelectric response obtained from a periodically poled RTP composed of inverted domains of about 5 μm wide strips spatially separated by a distance of around 15 μm. These types of images clearly revealed the existing 1D periodic patterns that correlate well to the alternating domain structure fabricated by DEWB with very good spatial control at the micrometer scale along the ***a*** direction.

The photoinduced silver nanoparticles deposition was carried out according to the previously described procedure for other ferroelectric crystals by illuminating with above-band-gap light at 254 nm the periodically poled RTP crystals immersed in an $AgNO_3$ solution.[17,18,25] The specific details on the procedure are given at the experimental section. Optical images of DIC and piezoelectric microscopy obtained after the procedure are displayed in Figures 1 (c) and (d), respectively. The comparison between the inverted regions before and after the metallization processes reveals a clear effect of the photochemical process on the ferroelectric domain structure. Namely, the self-formation of ferroelectric domain sub-structures can be clearly distinguished in both the optical and electrical micrographs. The domain sub-structures are parallel to the domains fabricated by DEBW and appear at all the inverted regions. The electrical nature of these substructures is clearly evidenced through the PFM images; no topographical structure was observed in the AFM images. Similar domain sub-structures have been recently reported in the isostructural Rb-doped KTP crystal when

electrical poling using liquid KCl electrodes after a chemical treatment was performed. The physical reason underlying this sub-domain formation is out of the scope of this manuscript, though changes in the stoichiometry of the surface layer and ionic conductivity after the photochemical treatment can be suggested as reversal domain nucleation mechanism according to Zukauskas *et al.*[26] Finally, Figures 1 (e) and (f) correspond to the SEM images showing the silver nanostructures on the alternating polarity domain surfaces. Silver is domain-selective and clearly follows the sub-μm domain structure formed in the RTP crystal. It occurs mainly on ***c***+ domain surfaces ~~as in other different ferroelectric crystals~~. This behavior is similar to that observed in other different ferroelectric crystals,[17,25] and has been related to polarization induced band bending at ferroelectric surfaces. [27]

Detailed images of the silver nanostructures on the RTP polar surface are shown in **Figures 2**(a) and (b). As clearly seen silver is deposited mainly in the shape of nanocubes. These nanocubes ~~are nearly monodisperse showing~~ show an edge length of 57 ± 6 nm, according to the Gaussian distribution of Figure 2(c). Here it should be mentioned that the presence of these regular nanocubes contrasts with previous results obtained for photo-deposition of metallic nanostructures on other ferroelectric crystal structures (PZT, $BaTiO_3$, $LiNbO_3$, ...) where mostly spherical-like metal nanoparticles and metallic nanowires have been obtained by using the same procedure.[17, 25, 28] Further, the obtained nanocubes exhibit a certain degree of orientation on the RTP substrate. Figure 2(d) shows a histogram with the orientation distribution corresponding to 250 nanocubes. Three preferential directions at around 0º and around ±40º with respect to the crystallographic ***b*** axis are observed. Both well-defined shape and orientations of the metal nanostructures suggest the possibility of epitaxial growth of metallic silver cubes on the polar surface of the RTP crystal, which could be justified by the crystal structure.

At room temperature the RTP belongs to the orthorhombic crystal system with a non-centrosymmetric space group $Pna2_1$ and point group *mm*2. The lattice parameters are *a* =

12.974, *b*= 6.494 and *c*= 10.691 Å, the *c* axis being the direction of the spontaneous polarization.[29,30] The crystal structure may be described as a network of distorted TiO_6 octahedra forming helical chains along the ***c*** direction. The Ti octahedra are linked by PO_4 tetrahedra along the ***a*** direction and along the ***a***-***c*** diagonal. The three-dimensional framework has large channels in which two nonequivalent Rb^+ ions (eightfold and ninefold coordinated) are accommodated, weakly bounded to the octahedra and tetrahedra groups. Figure 2(e) shows the projection of the crystal structure on the polar surface, which may act as platform for the silver deposition, preferentially into a cubic shape. There, the unit cell has been represented with dashed lines. The projection shows a multi-square-like grid atomic arrangement of slightly distorted square units, formed by oxygen or/and rubidium ions at the corners and centers, which can fit the lattice parameter of the metallic fcc silver structure, 4.086 Å. Two differently oriented solid squares with side lengths corresponding to the Ag lattice constant are superimposed on the picture of the polar face to illustrate the suitability of the RTP lattice for an epitaxial deposition of [100] oriented silver nanostructures with cubic morphology. The dominant orientation experimentally obtained for the nanocubes (0º with respect to the ***b*** axis) coincides with the ***a*** and ***b*** crystallographic directions of the RTP structure. Other preferential directions (±40º with respect to ***b*** axis, see Figure 2d) are close to the diagonal of the ***a***-***b*** plane. The distortion of the TiO_6 octahedra typical of KTP family polar structures,[31] which may vary with the partial substitution of rubidium by silver, together with the mismatch between the atomic positions at the RTP polar surface and the Ag (100) surface could justify the observed disorientation. A deeper analysis is needed to confirm the viability of the suggested epitaxial growth as well as to determine the possible Ag adsorption sites on the RTP substrate.

Once the selective deposition of Ag metallic nanocubes on the alternate ferroelectric domain structures on RTP is demonstrated, their role to enhance second harmonic generation (SHG) in the blue spectral region is evaluated. An optical characterization of the nonlinear

response was carried out by using a confocal microscope. In our experiments, the fundamental laser beam, tuned in the near-infrared region at ~840nm, was launched along the ***c*** polar axis and the backscattered SHG blue light at ~420 nm was collected in the same direction. According to the symmetry of the nonlinear tensor,[32] no SHG from bulk RTP should be observed for an incident beam along the ***c*** direction (z axis of the dielectric tensor). However, our experimental configuration allows the analysis of the far-field second harmonic emitted light that can be generated by the presence of nanoscale interfaces, in particular, domain wall surfaces. Therefore, the plasmonic effect of the silver nanocubes on the SHG from domain wall surfaces can be analyzed by comparing the performance before and after the silver deposition. **Figure** 3(a) (top) shows a 3D map of the integrated SHG response from the crystal surface of our periodically poled RTP crystal before the metallic deposition. As observed, SHG occurs mainly at domain walls following the pattern of the inverted ferroelectric domain structure fabricated by DEBW. The observation of SHG from the domain walls is associated with changes in the nonlinear properties around the domain boundaries which impose interface selection rules breaking those of the bulk crystal structure.[33,34]

The spatial map at the bottom of Figure 3a shows the integrated SHG response arising from the surface of the hybrid metal-ferroelectric heterostructure. A much more intense SHG response is obtained due to the presence of the silver nanocubes. The obtained SHG profile displays a modulation showing the effect of the aforementioned ferroelectric domain sub-structure appearing during the photochemical reduction process at the inverted regions. At these regions the density of domain boundaries separating positive and negative surfaces is higher resulting in a remarkable intensification of the SHG when the silver nanocubes are selectively grown on the alternating polar sub-structures. The generated blue SHG spectra at a single domain wall recorded before and after the deposition of the silver nanocubes are displayed in Figure 3(b). As observed, the SHG signal is increased by a factor of ~3. The intensification effect can be related to resonances between the LSP modes of the metallic

nanocubes and the nonlinear optical response of the RTP crystal. In fact, the fundamental beam was tuned so that the SH emission matches the region of the LSP resonance of 50 nm silver nanocubes which is centered at around 450 nm *i.e*, the blue spectral region.[13]

To further optimize the behavior of the system different configurations of metal nanoparticles are proposed. For instance, alternative configurations formed by aggregates of nanocubes, with absorption in the near infrared region (at around 800 nm)[35,36] could produce an intensification of the field intensity of the fundamental beam and therefore, a much greater enhancement of the SHG due to the two photon character of the nonlinear process. Such configurations could be obtained, for instance, by increasing the illumination time and/or the solution concentration.

In conclusion, for the first time the fabrication of alternate domain structures in a millimeter-thick RTP crystal by direct electron beam writing has been demonstrated. Afterwards, silver nanoparticles are selectively photo-deposited mainly on the positive ferroelectric domains surfaces. It is shown that silver directly forms ~~relatively monodisperse~~ regular nanocubes with an edge length of 57 ± 6 nm on the polar RTP surface without further processing. The multi-square symmetry of the RTP surface plus the fact that nanocubes preferentially orient along certain crystal orientations suggest epitaxial growth of silver into well-shaped fcc cubes. The excitation of local surface plasmons of the silver nanocubes, resonant with the quadratic nonlinear signal, leads to clear magnification of the SHG in the blue spectral region, which is of technological interest. An intensification by a factor of 3 is obtained, which is susceptible to be further improved by optimized nanoparticles distribution. Our novel approach constitutes a proof-of-principle for low-cost nanoplasmonics using specific ferroelectric surfaces and offers a suitable alternative to the usual colloidal routes for fabrication of targeted metal nanoparticles, which even might allow manufacture of scalable metamaterials. Epitaxial growth may provide a crucial advantage for selective orientation of

the nanocubes, and for their subsequent self-assembly into superstructures in which the ferroelectric surface acts as template.

Experimental Section

RTP single crystals were grown through the top-seeded solution growth (TSSG) method from high temperature. Solutions with a composition Rb_2O-TiO_2-P_2O_5-WO_3 = 42.24-16.80-18.96-20.00 mol% were prepared from Rb_2CO_3, TiO_2, $NH_4H_2PO_4$ and WO_3 precursors in 125 cm^3 cylindrical Pt crucibles. WO_3 was added to the solutions to reduce their viscosity and to facilitate the growth process. A ***c***-oriented crystal seed, located on the surface of the solution and on the axis of the Pt crucible, was used for the growth of RTP crystals. The crystal seed was rotated at an angular speed of 45 rpm to favor the homogenization of the solution of growth, and avoid the formation of flux inclusions in the crystals. The *a* crystallographic direction of the seed was always placed in the radial direction of the rotation movement. Further details on the crystal growth procedure can be found in reference.[37] The crystallographic orientation of the samples was controlled during the preparation process and confirmed by X-ray diffraction. For the experiments 3,8 mm x 11,7 mm x 1,3 mm (*x, y, z*) samples were prepared by slicing and polishing the single crystals obtained where *x*, *y* and *z* correspond to the crystallographic axis ***a***, ***b*** and ***c*** axes, respectively.

Prior to the deposition of Ag nanoparticles, periodically poled patterns with positive and negative domains with 180º domain boundaries were fabricated by direct electron beam writing. The electron beam from a scanning electron microscope was focused on the ***c***-surface of the RTP crystals. The procedure was performed by means of a Phillips XL30 Schottky field emission gun electron microscope driven by an Elphy Raith nanolitography software. Details can be found elsewhere.[22] The main irradiation parameters were: an acceleration voltage of 15kV and a beam current of ~450 pA. The charge density was in the

range 50 μC/cm^2 to 1000 μC/cm^2. In all the cases, ferroelectric domain inversion was achieved while maintaining the crystal quality. That is, the charge doses used to reverse the spontaneous polarization did not affect the inherent ferroelectric features of the material, which includes the spontaneous polarization value and therefore the surface charge of the crystals. The periodicity of the alternate polar structures varied from 5 to 50 μm and the width of the inverted domain ranged from 5 to 20 μm. The inverted domains were directed along the ***c*** polar axis of the crystal and crossed the whole thickness of the sample (1.3 mm). The electric characterization of the ferroelectric domain patterns was performed by means of piezo-response force microscopy (PFM), using an AFM Park Systems XE-100 provided with an electrostatic force microscopy module.

The photoinduced silver deposition process was carried out by illuminating the surface of the ***c*** -cut RTP crystal with a mercury lamp (main line at 253.6 nm), while the crystal was immersed in a 0.01M $AgNO_3$ solution without any additional surfactant nor capping agents. The emission power of the lamp was 5400 μWcm^{-2} at a distance of 2 cm. The illumination time was 2 min. SEM analysis by using a Philips XL30 Schottky field emission gun electron microscope supports the size and shape of the silver nanocubes, including the height. The experimental limitations of tilted SEM images together with the low density of silver nanocubes in our system prevent to perform any statistics on the height variation.

Far-field SHG experiments were performed in a laser scanning confocal microscope. A femtosecond Ti:sapphire laser (3900S Tsunami Spectra Physics) tuned at 840 nm was used as a fundamental beam. The laser was focused onto the sample by a microscope objective (50x magnification). Backscattered SHG light at around 420 nm was collected with this same objective. The samples were placed on a two-axis XY motorized stage in order to register a map of the SHG radiation from the periodically poled RTP crystals. The spatial resolution of the stage was 0.1 μm.

Acknowledgements
This work has been supported by the Spanish Government under projects MAT2010-17443, MAT2011-29255-C02-02 and MAT2013-43301-R, Comunidad de Madrid under grant S2009/1756 and Generalitat de Catalunya under project 2009SGR235

Received: ((will be filled in by the editorial staff))
Revised: ((will be filled in by the editorial staff))
Published online: ((will be filled in by the editorial staff))

[1] W. L. Barnes, A. Dereux, T. W. Ebbesen, *Nature* **2003**, *424*, 824.

[2] E.Hutter, J.H. Fendler *Adv.Mat.* **2004**, *16*, 1685-1706

[3] A. D. McFarland, R. P. Van Duyne, *Nano Lett.* **2003**, 3, 1057.

[4] S.A Maier, P.G Kik, H.A Atwater, S. Meltzer, E. Harel, B. E. Koel, A.A.G. *Nat. Mater.* **2003**, *2*, 229-232.

[5] M. W. Knight, H. Sobhani, P. Nordlander, N. J. Halas, *Science* **2011**, 332, 702.

[6] H. A. Atwater, A. Polman, *Nat. Mater.* **2010**, 9, 205.

[7] M. A. Noginov, G. Zhu, A. M. Belgrave, R. Bakker, V. M. Shalaev, E. E. Narimanov, S. Stout, E. Herz, T. Suteewong, U. Wiesner, *Nature* **2009**, 460, 1110.

[8] O. Hess, J. B. Pendry, S. A. Maier, R. F. Oulton, J. M. Hamm, K. L. Tsakmakidis, *Nat. Mater.* **2012**, 11, 573.

[9] L. Novotny, N. van Hulst, *Nat. Photonics* **2011**, 5, 83.

[10] H. Wang, Y. P. Wu, B. Lassiter, C. L. Nehl, J. H. Hafner, P. Nordlander, N. J. Halas, *Proc. Natl. Acad. Sci. U. S. A.* **2006**, 103, 10856.

[11] E. Carbo-Argibay, B. Rodriguez-Gonzalez, J. Pacifico, I. Pastoriza-Santos, J. Perez-Juste, L. M. Liz-Marzan, *Angew. Chem. Int. Ed.* **2007**, 46, 8983.

[12] M. Grzelczak, L. M. Liz-Marzan, *Langmuir* **2013**, 29, 4652.

[13] L. J. Sherry, S. H. Chang, G. C. Schatz, R. P. Van Duyne, B. J. Wiley, Y. N. Xia, *Nano Lett.* **2005**, 5, 2034.

[14] A. Moreau, C. Ciraci, J. J. Mock, R. T. Hill, Q. Wang, B. J. Wiley, A. Chilkoti, D. R. Smith, *Nature* **2012**, 492, 86.

[15] L. M. Liz-Marzan, *Langmuir* **2006**, 22, 32.

[16] V. Gopalan, K. L. Schepler, V. Dierolf, and I. Biaggio, in *The Handbook of Photonics*, 2nd Edition (Eds: J. Ballato and M.C Gupta), CRC Press, Boca Raton, FL **2006** , Ch. 6.

[17] S. V. Kalinin, D. A. Bonnell, T. Alvarez, X. J. Lei, Z. H. Hu, R. Shao, J. H. Ferris, *Adv. Mat.* **2004**, 16, 795.

[18] Y. Sun, R. J. Nemanich, *J. Appl. Phys.* **2011**, 109, 104302.

[19] H. Karlsson, F. Laurell, L. K. Cheng, *Appl. Phys. Lett.* **1999**, 74, 1519.

[20] Y. Guillien, B. Menaert, J. P. Feve, P. Segonds, J. Douady, B. Boulanger, O. Pacaud, *Opt. Mater.* **2003**, 22, 155.

[21] C. Canalias, J. Hirohashi, V. Pasiskevicius, F. Laurell, *J. Appl. Phys.* **2005**, 97, 124105.

[22] L. Mateos, L. E. Bausa, M. O. Ramirez, *Appl. Phys. Lett.* **2013**, 102, 042910.

[23] L. Mateos, M. O. Ramírez, I. Carrasco, P. Molina, J. F. Galisteo-López, E. G. Víllora, C. de las Heras, K. Shimamura, C. Lopez, L. E. Bausá, *Adv. Funct. Mater.* **2014**, 24, 1509.

[24] G. Rosenman, P. Urenski, A. Agronin, A. Arie, Y. Rosenwaks, *Appl. Phys. Lett.* **2003**, 82, 3934.

[25] E. Yraola, P. Molina, J. L. Plaza, M. O. Ramirez, L. E. Bausa, *Adv. Mat.* **2013**, 25, 910.

[26] A. Zukauskas, V. Pasiskevicius, C. Canalias, *Appl. Phys. Lett.* **2013**, 103, 252905.

[27] S.V Kalinin, D.A. Bonnell, T.Alvarez, X.Lei, Z. Hu, J.H. Ferris, *Nano Lett.* **2002**, 2, 589.

[28] J. N. Hanson, B. J. Rodriguez, R. J. Nemanich, A. Gruverman, *Nanotechnology* **2006**, 17, 4946.

[29] I. Tordjman, R. Masse, J. C. Guitel, *Z. Kristallogr.* **1974**, 139, 103.

[30] J. D. Bierlein, H. Vanherzeele, *J. Opt. Soc. Am. B-Opt. Phys.* **1989**, 6, 622.

[31] J. D. Bierlein, F. Ahmed, *Appl. Phys. Lett.* **1987**, 51, 1322.

[32] M. V. Pack, D. J. Armstrong, A. V. Smith, *Appl. Opt.* **2004**, 43, 3319.

[33] S. I. Bozhevolnyi, J. M. Hvam, K. Pedersen, F. Laurell, H. Karlsson, T. Skettrup, M. Belmonte, *Appl. Phys. Lett.* **1998**, 73, 1814.

[34] A. Fragemann, V. Pasiskevicius, F. Laurell, *Appl. Phys. Lett.* **2004**, 85, 375.

[35] V. Bastys, I. Pastoriza-Santos, B. Rodriguez-Gonzalez, R. Vaisnoras, L. M. Liz-Marzan, *Adv. Funct. Mater.* **2006**, 16, 766.

[36] B. Gao, G. Arya, A. R. Tao, *Nat. Nanotech.* **2012**, 7, 433.

[37] J. J. Carvajal, R. Sole, J. Gavalda, J. Massons, M. Aguilo, F. Diaz, *Crystal Growth & Design* **2001**, 1, 479.

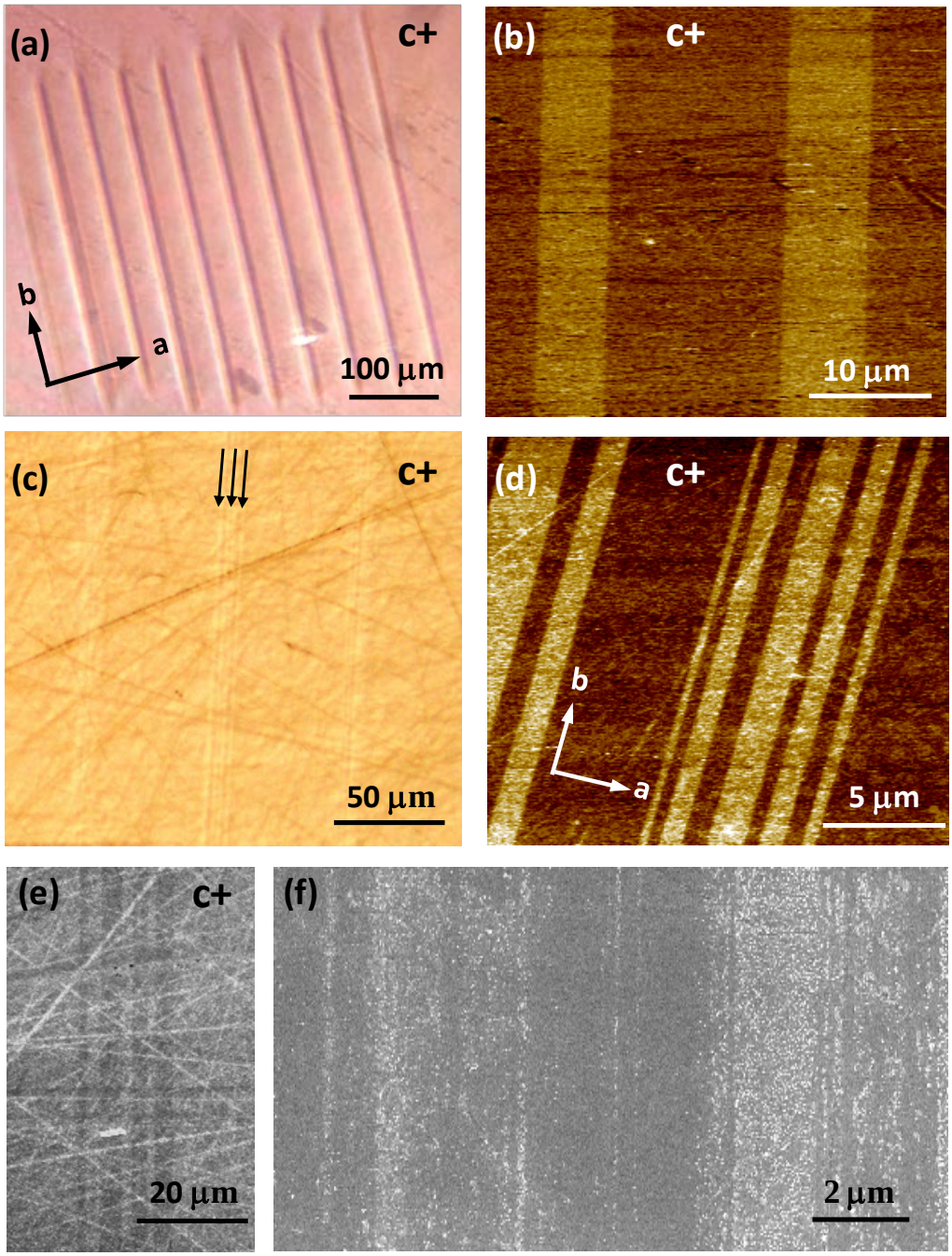

Figure 1. (a) DIC micrograph and (b) PFM image of two ferroelectric domain patterns obtained by DEBW in RTP. The inverted domains are 10 µm width separated 30µm (a) and 5µm width separated 15 µm (b). (c) DIC micrograph and (d) PFM image showing the domain sub-structure appearing in the ferroelectric pattern after the silver photo-deposition. (e) and (f) SEM images showing the domain-selective deposition of silver nanostructures on the ***c+*** surface of RTP.

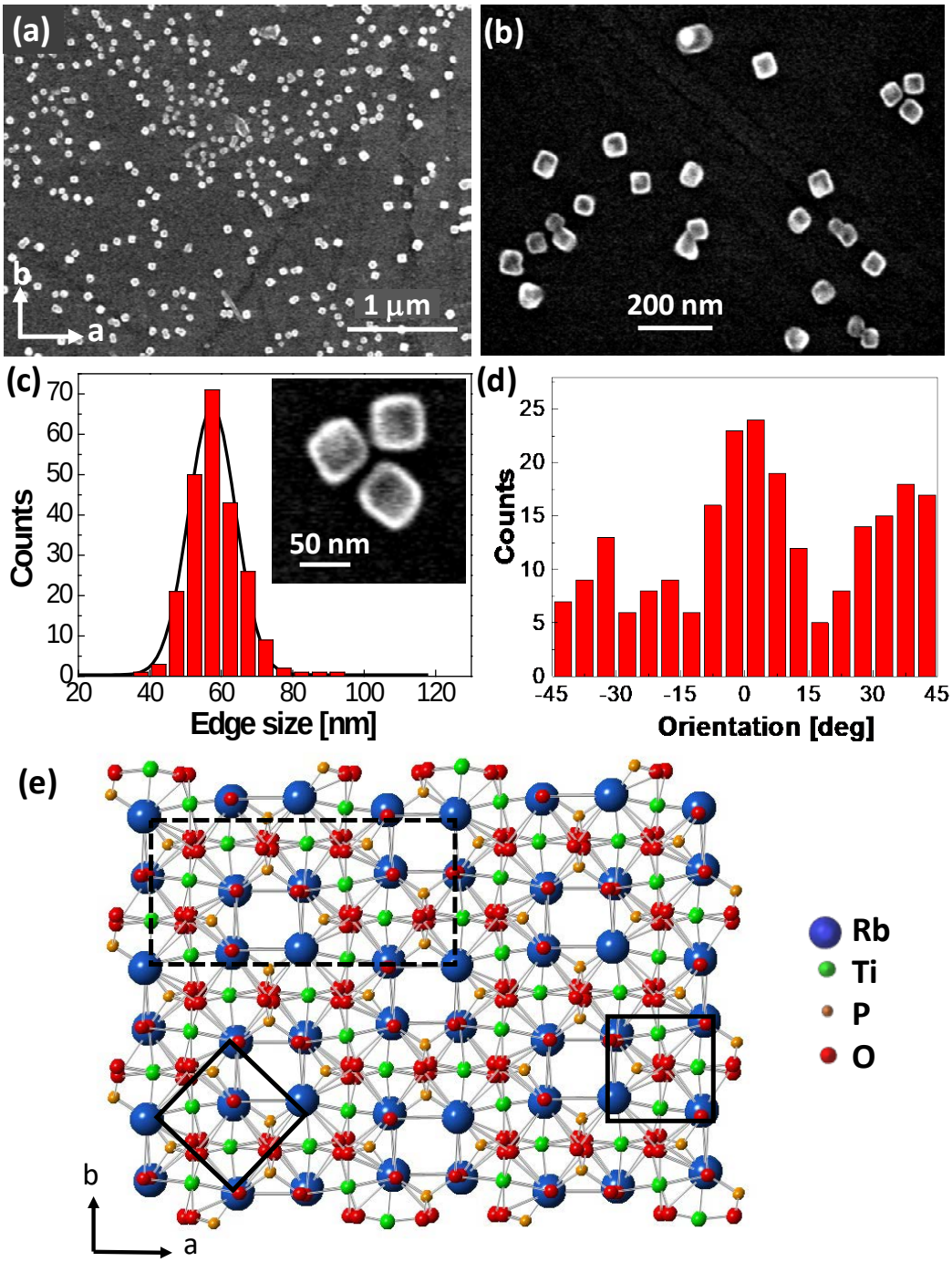

Figure 2. (a) and (b) SEM images of silver nanocubes photochemically deposited on the ***c***+ surface of RTP. The obtained nanocubes ~~are nearly monodispersed and~~ show preferential orientations with respect to the ***b*** axis. (c) Histogram and Gaussian distribution of the edge sizes of the nanocubes showing an average value of 57 ± 6 nm. The inset corresponds to a detailed SEM image showing 3 nanocubes with an edge size of around 50 nm. (d) Orientation distribution corresponding to 250 cubes. Three preferential orientations corresponding to crystal directions at 0º and around ±40º with respect to the ***b*** axis are observed. (e) Projection of the RTP crystal structure on the polar surface. The unit cell of RTP is marked in dashed lines. The solid black squares represent the (100) sides of the silver unit cell oriented at 0º and 45º with respect to the RTP crystal axis.

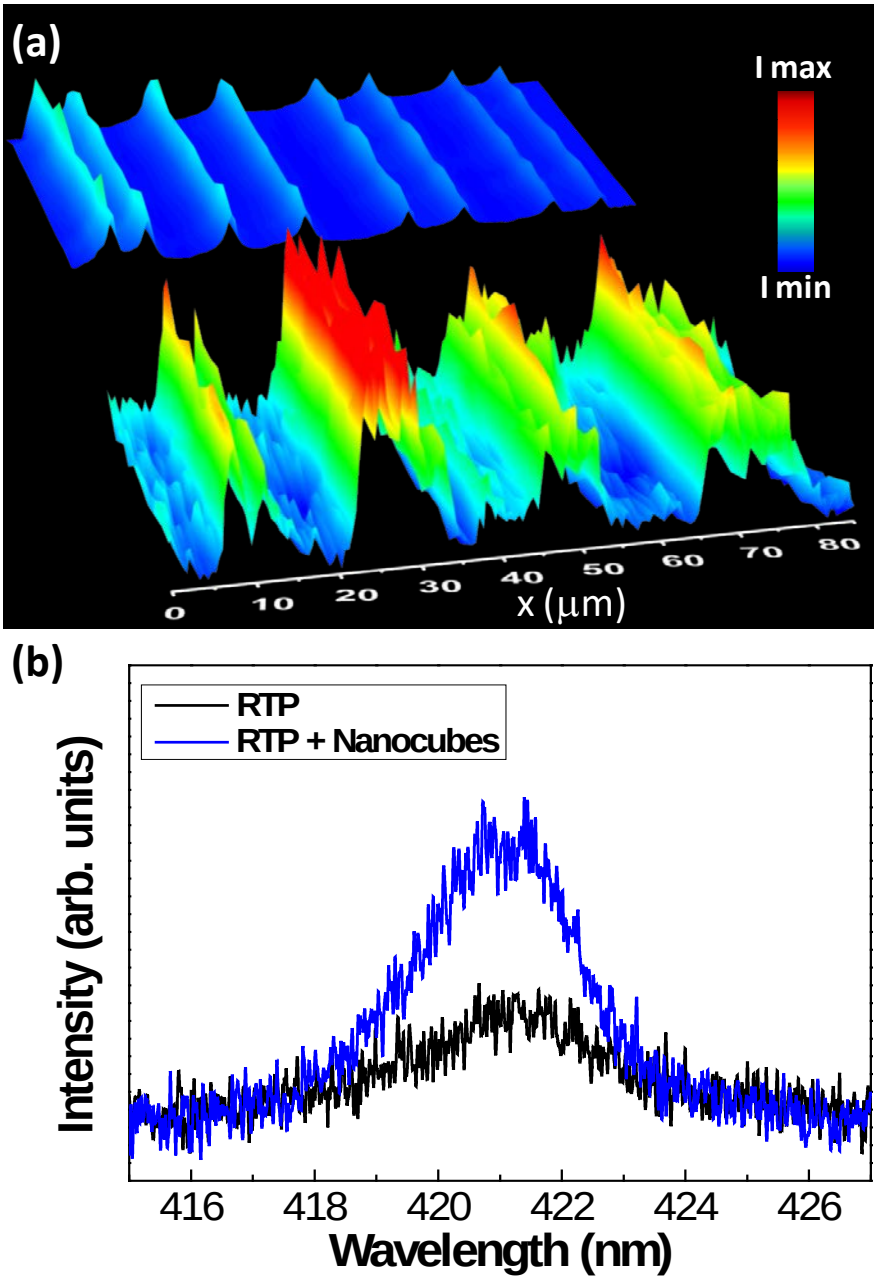

Figure 3. (a) Spatial distribution of the integrated blue SHG at the domain wall surfaces in a periodically poled RTP with a period of around 20 μm before (top) and after (down) photo-deposition of silver nanocubes. The effect of the silver photo-deposition produces an increment in the number of domain walls as well as an intensification of the generated blue SHG from each wall. (b) SHG spectra from the surface of a single domain wall before and after the silver nanocubes deposition.